Measurement of the muon capture rate in gaseous hydrogen

V. M. Bystritskiĭ, V. P. Dzhelepov, P. F. Ermolov,[1] K. O. Oganesyan, M. N. Omel'yanenko, S. Yu. Porokhovoĭ, V. S. Roganov, A. I. Rudenko, and V. V. Fil'chenkov

Joint Institute for Nuclear Research
(Submitted July 25, 1973)
Zh. Eksp. Teor. Fiz. **66**, 43–60 (January 1974)

Muon capture by protons (1) has been studied with a gaseous hydrogen target in the muon beam of the JINR synchrocyclotron. 278±33 events of this type were recorded. The measured capture rate is $\lambda_{capt}^{p\mu}=686\pm88\ sec^{-1}$. The result agrees with the predictions of the universal four-fermion interaction theory and definitely favors the *V-A* variant of this theory.

1. INTRODUCTION

Experimental study of the capture of muons by protons

$$\mu^-+p\rightarrow n+\nu_\mu \qquad (1)$$

presents substantial interest in weak-interaction physics. According to the theory of the universal four-fermion interaction, weak processes, including μ capture, β decay

$$n\rightarrow p+e^-+\bar{\nu}_e \qquad (2)$$

and muon decay

$$\mu\rightarrow e+\nu+\bar{\nu}, \qquad (3)$$

should be described identically by a mixture of vector (V) and axial (A) interactions with "bare" coupling constants equal in magnitude and opposite in sign, $g_V^0=-g_A^0$. Verification of this statement would have fundamental importance.

The participation of strongly interacting particles in processes (1) and (2) leads, on the one hand, to renormalization of the coupling constants (it actually turns out that only the axial constant is renormalized, so that $g_A^\beta=-1.23\ g_V^\beta$) and, on the other hand, to appearance of induced interactions: "weak magnetism" and an "induced pseudoscalar" interaction with coupling constants g_M and g_P. In view of the fact that substantially more energy is released in process (1) than in process (2), the contribution of induced interactions in μ capture becomes significant and should appreciably affect the probability of absorption of the muon by a proton.

Up to the present time the task of experimentally verifying the ideas of the current theory of μ capture by a proton cannot be considered completed, as a result of the great difficulties in studying this process in hydrogen. At the same time the use of data on μ capture in complex nuclei for determination of the constants of the elementary process (1) is extremely unsatisfactory because of the inaccurate knowledge of the nuclear wave functions.

The basic results of calculations of the rate $\lambda_{capt}^{p\mu}$ of muon capture from a state of the hydrogen mesic atom are contained in refs. 1–3. We note that the capture rate from the triplet state of the $p\mu$ atom is very small and amounts to

$$\lambda_{capt}^{p\mu}(F=1)=12\ sec^{-1} \qquad (4)$$

(here F is the total spin of the $p\mu$ atom). According to the most complete theoretical study[3] the value $\lambda_{capt}^{p\mu}$ (F = 0) is

$$\lambda_{capt}^{p\mu}(F=0)=654\ sec^{-1}; \qquad (5)$$

it is given in Table I. It should be emphasized that this rate is about 700 times less than the rate $\lambda_0=4.55\times10^5\ sec^{-1}$ of decay of the muon, which is the main channel for loss of the muon in the $p\mu$ atom. This low probability for process (1) in hydrogen substantially hinders investigation of the process.

Because of the great experimental difficulties, the first experiments on measurement of the reaction (1) rate were carried out with liquid hydrogen. The results of these experiments are shown in Table I. It is important that in liquid hydrogen capture occurs preferentially from a state of the mesic molecular ion $(pp\mu)^+$, since the rate $\lambda_{pp\mu}$ of formation of this system under conditions of high hydrogen density is several times greater than the rate of muon decay.[9-11] The rate $\lambda_{capt}^{pp\mu}$ of muon capture in the $(pp\mu)^+$ system can be expressed[1,12] in terms of the capture rate in the $p\mu$ atom:

$$\lambda_{capt}^{pp\mu}=2\gamma\left[{}^3/_4\xi\lambda_{capt}^{p\mu}(F=0)+(1-{}^3/_4\xi)\lambda_{capt}^{p\mu}(F=1)\right]. \qquad (6)$$

Here γ and ξ are mesic molecular parameters associated with overlap of the proton and muon wave functions and with the relative orientation of the spins of these particles. Values of the capture rate in liquid hydrogen calculated with inclusion of the latest calculations[2,13]

TABLE I. Muon capture rate in hydrogen

Experiment		Theory	
Source of data	λ_{capt}, sec^{-1}	Source of data	λ_{capt}, sec^{-1}
Liquid Hydrogen			
[4]	428±85	[2]	516±22 *
[5]	450±50		
[6]	464±42	[2]	498±21 *
Gaseous Hydrogen			
[7]	651±57	[3]	654
Present work	686±88		

*The data were taken from the work of Kabir[2] and corrected (by 5%) on the basis of the latest results on determination of g_A/g_V in β decay.[8] Kabir's calculations[2] took into account that under the experimental conditions of refs. 4 and 5 (bubble chamber) the capture occurs partly from a state of the mesic atom, while in experiments in which neutrons are detected with a delay of 1 μsec, muon capture occurs almost entirely from a state of the mesic hydrogen molecule.[6]

Copyright © 1975 American Institute of Physics

of γ and ξ ($2\gamma = 1$, $\xi = 1$) are given in the last column of Table I. As can be seen, satisfactory agreement is observed of the experimental results with the theoretical predictions. It is important, however, to emphasize that the very methods of calculating γ and ξ are approximate (as referred to three-body problem), which leads to an uncertainty in the interpretation of the data on μ capture in liquid hydrogen.

In this situation it is extremely urgent to have experiments on process (1) under conditions where the rate of production of $(pp\mu)^+$ is substantially smaller, i.e., in gaseous hydrogen. It has already been established[14,15] that a $p\mu$ atom formed in a statistical mixture of spin states ($F = 1, 0$) rapidly transfers to the singlet state ($F = 0$) as the result of specific mesic-atom processes. The transition time in gaseous hydrogen is two to three orders of magnitude shorter than the lifetime of the $p\mu$ atom, and therefore μ capture under these conditions occurs practically only from the state with $F = 0$.

At the present time only one paper[7] is known on the experimental measurement of the muon capture rate in gaseous hydrogen. In view of the importance of the problem being studied, we attempted to obtain independent data for the rate of process (1) in measurements carried out by another method.

2. DESIGN OF THE EXPERIMENT AND BASIC FEATURES OF THE METHOD

The design of the experiment reduces in principle to the following. Muons stop and form mesic atoms in a gaseous hydrogen target. Neutrons from capture of muons are detected by scintillation counters located around the target. Detection of the neutrons is accomplished in a time gate triggered by the muon stopping signal.

The principal experimental difficulties are due mainly to the extremely low probability of the process being studied, the low intensity of muon stoppings in hydrogen, and consequently the relatively low neutron counting rate from μ capture in the presence of a large background of various processes. In preparation of the experiment and the apparatus we strove to provide conditions such that the background level would be sufficiently small. The main features of the method are listed below.

1. To reduce the accidental-coincidence background, the experimental apparatus was placed in a specially built laboratory with a low background and in addition was surrounded by a water shield.

2. To remove the "wall effect"—the background of neutrons from muon capture in the target walls—muon stoppings were identified by means of a scintillator located inside the target.

3. To avoid background from μ capture in possible impurities contained in the hydrogen, the experiments were performed with ultrapure hydrogen obtained by means of a specially built apparatus with a palladium filter.[16]

4. To discriminate against the γ-ray background (accidental coincidences and bremsstrahlung from electrons produced in muon decay), neutrons and γ rays were separated on the basis of the pulse shape in the scintillator of the neutron detector.

5. The complex of experimental apparatus was connected to a Minsk-22 computer to provide constant monitoring of the state of the equipment during extended runs and to obtain information during the operation.

3. APPARATUS

A diagram of the main portion of the apparatus (the target and the neutron detectors) is shown in Fig. 1. The muon beam of the JINR synchrocyclotron was used to channel a 130-MeV/c muon beam into the low-background laboratory where the experimental equipment was located. The muons were slowed down by an absorber 1 and stopped in a gas target.

The target was a stainless steel vessel 540 mm long with an internal diameter of 140 mm and a wall thickness of 3 mm. Scintillators of CsI(Tl) were placed inside the target to identify muon stoppings. One of these scintillators was made in the form of a flat-bottomed cylindrical vessel with internal diameter 120 mm, length 205 mm, and wall thickness 5 mm, and the other scintillator, adjacent to the first, consisted of a 120 mm in diameter and 250 microns thick. The light from the scintillations was carried to photomultipliers by means of hollow light pipes 2 and transparent seals.

Although CsI(Tl) has poorer time resolution properties than plastic scintillators, it was chosen particularly for identification of muon stoppings inside the target. This choice was dictated by two circumstances. First, the muon lifetime in CsI(Tl) is only 0.09 μsec, and therefore the background of neutrons from muon capture in this material can be easily discriminated against by introduction of a delay in the neutron-detection channel. Second, the level of gas evolution (release of absorbed water vapor and other gases) for plastic scintillators turned out to be unacceptably high from the point of view of preserving the necessary purity of the hydrogen.

To provide the necessary purity of the hydrogen we constructed and used a system which included an apparatus for diffusion purification of the hydrogen (a palladium absorber), vacuum pumps, absorption traps, and other elements. A detailed description of this equipment has been given previously.[16,17] Before measurements were made in the muon beam the target, palladium absorber, and all connecting lines were con-

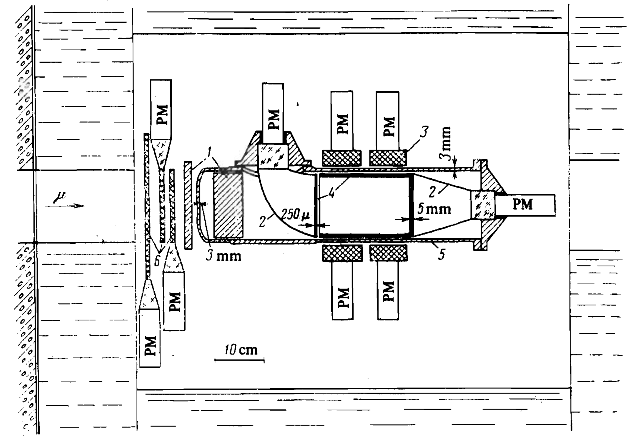

FIG. 1. Diagram of the main part of the experimental equipment (gas target and neutron detectors): 1) copper absorber, 2) hollow light pipe, 3) stilbene crystal, 4) CsI(Tl) scintillator, 5) stainless steel body of target, 6) plastic scintillator.

tinously pumped for seven or eight days to assume an acceptably low level of contamination of the hydrogen in the target as the result of gas evolution. Our control analyses[17] of the hydrogen purity in the target showed that the relative content of impurities with $Z > 1$ was no more than 10^{-8} parts by volume, and this degree of purity was preserved during the time occupied by the series of measurements (about seven days).

Figure 2 is a block diagram showing the connections of the counters and electronic equipment. The technique of identifying muon stoppings by means of CsI(Tl) scintillators has been described in an earlier article.[18] The muon stopping signal was a $234\bar{5}$ coincidence pulse. The number of these pulses was approximately 1.5 times the number of stoppings in the hydrogen; this excess is due mainly to muon stoppings in the scintillator of counter 4. The muon stopping pulse ($234\bar{5}$) triggered a gate delayed by 1.3 μsec and of duration 4 μsec, during which events recorded by the neutron detectors were analyzed.

The multichannel neutron-detection system has also been described previously.[19] The neutron detectors were nine scintillation counters with stilbene crystals of diameter 70 mm and thickness 30 mm (neutron detection was accomplished by means of the recoil protons). The pulses from the neutron-counter outputs were fed to the inputs of two blocks of electron circuits. One of these, the component separation block (CS), served to separate neutrons and γ rays on the basis of the shape of the light pulse in the stilbene. This block produced two pulses. The height of one of the pulses was proportional to the area of the fast component (FC) of the scintillator pulse, and the height of the other pulse was proportional to the total area of the light pulse, i.e., to the particle energy E on an equivalent-electron-energy scale. In the other block two pulses were also produced. One of these pulses (n) was a logic pulse and indicated that an event had been detected in one of the neutron counters; the height of the second pulse depended strictly on which counter detected the neutron. This pulse therefore characterized the number of the detector (No.) and was used to perform an analysis of the data separately for each detector. The spectrometric signals FC, E, and No. were fed to the inputs of a multidimensional pulse-height analyzer (MPA).[20] The fourth parameter in the multidimensional analysis was the time T of detection relative to the time of the muon stopping, measured for the logic signal n by means of a time-to-pulse-height converter ($T \rightarrow A$).

Analysis of the events recorded by the neutron detectors was permitted by the logic only under the following conditions:

a) No second muon is detected by counter 1 in a period 6 μsec before and 6 μsec after the stopping signal. This condition is introduced to discriminate against accidental-coincidence background due to the muon beam.

b) In the same time interval there were no "fast" coincidences (with a resolving time ≈ 1 μsec) for the pulses of counter 1 and the n pulses. This condition assured discrimination against the background due to muon stoppings in the neutron-detector scintillators.

c) No more than one event was detected in a single triggering of the gate.

d) Events involving simultaneous detection by two or more neutron detectors were not analyzed.

e) No pulses were recorded in the anticoincidence counter 5 in the time interval of ± 6 μsec. This condition resulted in a substantial reduction of the accidental-coincidence background as the result of exclusion of gates due to detection of electrons from muon decay.

4. EXPERIMENTAL CONDITIONS

In all of the runs the coincidence counting rate for the monitor counters 2 and 3 was about 10^4 per second and for 234 coincidences about 10^3 per second. The hydrogen pressure in the target was set at 41 atm, and the number of muon stoppings in the gas was about 30 per second. The number of stoppings was determined by measurement of the yield of electrons in "electron" runs in which the blocking of triggers by the counter-5 channel was removed. In these runs counter 5 was used only to detect $234\bar{5}$ anticoincidences.

Table II gives the values of the detection efficiencies for neutrons (ϵ_n) and electrons (ϵ_e) by the neutron detectors. For electrons these values are given per muon decay in hydrogen, and for neutrons--per capture. Approximate values of the contribution of various factors to the efficiencies are given in the same table. The values of ϵ_n and ϵ_e were calculated by the Monte Carlo method on a BÉSM-6 computer. The calculations specified the spatial distribution of muon stoppings in the target volume as measured by us and the detector geometry, and also took into account the interaction of neutrons and electrons with the material of the target walls. The efficiency for neutron detection in stilbene was checked experimentally with an accuracy of 3–5% in experiments carried out in the ÉG-5 electrostatic generator at the Joint Institute for Nuclear Research. The two-deuteron fusion reaction was used as a source of monochromatic neutrons,

$$d+d \rightarrow He^3+n. \quad (7)$$

Monitoring was accomplished by use of a semiconductor

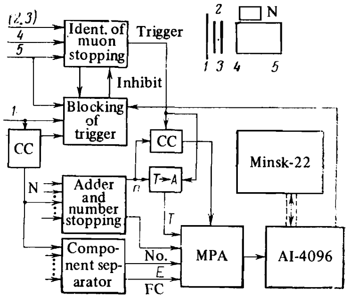

FIG. 2. Block diagram showing connection of the counters and electronic equipment (here CC are coincidence circuits, N is the neutron counter, and the remaining designations are given in the text).

TABLE II. Detection efficiency for neutrons and electrons by the neutron detectors

Parameter	Neutrons	Electrons
Solid angle	0.25	0.25
Time gate factor	0.46	0.46
Interaction efficiency in stilbene	0.18	1.00
Wall traversal coefficient	0.90	0.71
Threshold factor in pulse-height spectrum	0.42	0.92
Final efficiency value ϵ	0.007892±0.000331	0.07519±0.00195

detector to record protons from the second channel of this reaction,

$$d+d\to t+p. \quad (8)$$

The energy thresholds in our experiments were 0.78 MeV for neutron detection and 0.4 MeV for electron detection (on an equivalent-electron-energy scale). Under these conditions the rate of collection of the desired events from muon capture in hydrogen was about one event per hour.

We will consider questions related to the background level in our experiments.

A. Accidental coincidences

The blocking in the case of two muons (section 3, condition a) discriminates against the accidental-coincidence background due to capture of muons in the absorber, target walls, or scintillators. This background is almost entirely due to neutrons produced as the result of interaction of the accelerator proton beam with matter and penetrating through the shielding walls to the location of the experimental equipment. The results of measurements with an evacuated target and with a target filled with xenon show that accidental coincidences amount to $\approx 40\%$ of the total neutron counting rate in the experiments with hydrogen.

B. Spurious triggers from muon stoppings in the scintillators

The spurious triggerings are those which are not due to muon stoppings in the hydrogen. In view of the fact that the muon lifetime in CsI(Tl) is $\sim 0.09\ \mu$sec, introduction of the 1.3-μsec delay in the triggering of the neutron gates results in suppression of the background of neutrons from capture of muons in the scintillators of counters 4 and $\bar{5}$ by a factor $\leq 10^{-6}$, i.e., to a negligible level.

The background arising from muon capture in the scintillators of the neutron detectors cannot be discriminated against on the basis of time, since the muon lifetime in stilbene is $\approx 2\ \mu$sec. This background can be important, since the probability of capture in stilbene is two orders of magnitude greater than the probability of capture in hydrogen, and detection of the capture products occurs under conditions of a 100% solid angle. However, the appearance of spurious triggers from stopping of a muon outside the target is extremely unlikely because of the low accidental-coincidence rate in the $234\bar{5}$ count. In addition, these triggers from muon stoppings in the stilbene are further suppressed by blocking in the case of (1, n) coincidences. In order to determine the fraction of muons which stopped in the scintillators of the neutron counters, we measured the yield of electrons in experiments with an evacuated target and with the blocking on the basis of (1, n) coincidences turned off. The results of these measurements show that the contribution of background from capture of muons in stilbene was less than 1% compared to capture in hydrogen.

C. Background from muon capture in possible impurities in the hydrogen

We have already noted that the impurity content in the hydrogen in our experiments was less than 10^{-8}. The transfer rate $\lambda_{\text{trans}}^{\text{C,O}}$ from the pμ atom to such nuclei as C and O is[21] $\approx 5\times 10^{-9}\ \text{sec}^{-1}$ (recalculated to the density of liquid hydrogen), and therefore the relative number of mesic atoms Cμ and Oμ formed as the result of such transfer turns out to be less than 5×10^{-5} under our experimental conditions. If the distance (about 100 times) in the muon capture probabilities in hydrogen and in C and O is taken into account, the contribution of background from capture in impurities should be less than 0.5%.

The deuterium content in the hydrogen was $(1.5 \pm 0.5)\times 10^{-6}$. Since the rate of muon transfer into deuterium is of the order [9,22,23] of $10^{10}\ \text{sec}^{-1}$ (for the density of liquid hydrogen), the relative number of dμ atoms formed was less than 0.15%.

D. Background from diffusion of pμ atoms to the target walls

This background arises as the result of the following sequence of processes. pμ atoms diffusing in hydrogen reach the inner surface of the CsI scintillators (which are essentially the walls of the target). Muons are transferred from the pμ atoms to the nuclei of the scintillator materials and then are captured by these nuclei with emission of neutrons. The contribution of this background can be important, since the probability of muon capture in CsI is close to unity.

In order to obtain data on the fraction ($\alpha_{p\mu}$) of pμ atoms which reach the walls and also on the distribution in time of diffusion to the walls, we carried out calculations of the diffusion of pμ atoms in a computer by the Monte Carlo method. The calculations were based on the same assumptions as in ref. 15. The value of $\alpha_{p\mu}$ calculated by computer (for the cross section for elastic scattering of pμ atoms by protons found in ref. 15) turned out to be

$$\alpha_{p\mu}=9.9\cdot 10^{-3}. \quad (9)$$

If we use the data of refs. 24 on the yields and spectra of neutrons from μ capture in the region of nuclei near cesium and iodine and use the computer results for $\alpha_{p\mu}$ and also for the form of the distribution in diffusion time, we obtain for the relative contribution of the background from diffusion a value of the order 20–30%. In view of the fact that this contribution turns out to be so significant, we undertook special experiments to determine it.

E. Background from (γ, n) and (γ, p) reactions in stilbene

This background arises as the result of interaction of bremsstrahlung photons, emitted by electrons from muon decay, with carbon nuclei in the material of the neutron-detector scintillators. Estimates based on known data on photonuclear cross sections[25] show that this background can amount to 10–20% of the effect.

It is important that this background depends on the degree of discrimination achieved by means of counter 5 for those electrons which fall in the solid angle of the neutron detectors. This fact is also used to determine this background.

5. EXPOSURE IN THE MUON BEAM. SELECTION OF NEUTRON EVENTS

A total of four main experimental runs of length about 150 hours each were made in the muon beam. In each run, in addition to measurements with hydrogen, we measured the accidental-coincidence background in experiments with an evacuated target and with a target filled with xenon. The "neutron" measurements were periodically alternated with "electron" measurements in which the blocking by counter 5 was removed. Every 8–10 hours calibration measurements were made with γ sources and a Po-Be source. Some data which characterize the measurements under various conditions are shown in Table III.

Analysis of the experimental data was carried out directly during the runs by means of a Minsk-22 computer. Periodically every few hours the collection of data consisting of coded four-dimensional coordinates (FC, E, No., T) of the events were transferred to the computer and processed. The analysis in the computer was for the purpose of monitoring the state of the apparatus and selection of neutron events. For this purpose an ATsPU printer was used to extract one-dimensional amplitude spectra in E, No., and T. The parameters of these spectra were printed and two-dimensional distributions in the coordinate plane (FC, E) were constructed.[2)] The analysis process automatically determined by the method of least squares the parameters of the relativistic and nonrelativistic regions in the two-dimensional distributions and also the parameters of the line separating these regions. Figure 3 shows such a two-dimensional distribution measured for a Po-Be source. The points in this figure show the lines of the centers of gravity of the two regions and the line of separation. Figure 4 shows the same kind of distribution obtained in measurements of hydrogen.

Events belonging to the nonrelativistic region in the two-dimensional distributions were classified as neutron events, and those belonging to the relativistic region—as electron events. The total numbers of events obtained under various experimental conditions are given in Table III. The numbers of neutron events are given for the energy range 0.78–3.00 MeV, and the numbers of electron events for electron-energy values greater than 0.4 MeV. The nature of the electron pulse-height distribution is such that the number of events in the energy region 0.78–3.00 MeV is several times smaller than the total number of events. As a result the ratio of intensities of the electron and neutron regions for this energy range is ~10. Since the inefficiency in separation of neutrons and electrons[19] is no poorer than 10^{-3}, the background of γ rays (electrons) resulting from incomplete separation was no more than 1%. We determined the size of this background on the basis of the number of events lying near the line of separation of the two regions (±1 space on the printer) in the electron measurements and from the ratio of intensities of electron events in the two measurement modes—with an without blocking by counter 5.

6. EXPERIMENTS TO DETERMINE THE BACKGROUND FROM DIFFUSION OF $p\mu$ ATOMS

In order to determine the background from diffusion of $p\mu$ atoms, we undertook special experiments. The procedure for finding the background was as follows:

a) In experiments with hydrogen and pure helium we measured the yields of delayed γ rays. The difference in these yields, normalized to the number of muon stoppings, was interpreted as the field n_γ^H of γ rays (mainly mesic x radiation) arising in CsI(Tl) as the result of diffusion of $p\mu$ atoms.

b) We measured the ratio $(\eta_\gamma/\eta_n)_{CsI}$ of the yields of γ rays and neutrons arising in formation of mesic atoms of cesium and iodine and the subsequent capture of the muon in these mesic atoms.

c) The background δ_d of neutrons from diffusion, normalized to the number of stoppings, was determined as

$$\delta_d = \eta_\gamma^H (\eta_\gamma/\eta_n)_{CsI}^{-1}. \qquad (10)$$

Detection of γ rays was accomplished by means of a scintillation counter with a NaI(Tl) crystal, connected instead of one of the neutron detectors. The scintillator dimensions were 150 × 100 mm and the range of γ-ray energies measured was chosen from 1.5 to 7 MeV (the energy of the K_α line of mesic x rays for iodine is ≈4 MeV).

TABLE III. Yield of neutrons and electrons in runs with hydrogen

	Neutron runs	Electron runs
Total number of triggers	$27.34\cdot10^6$	$2.23\cdot10^6$
Number of neutron events	685	221
Number of electron events	23710	87320

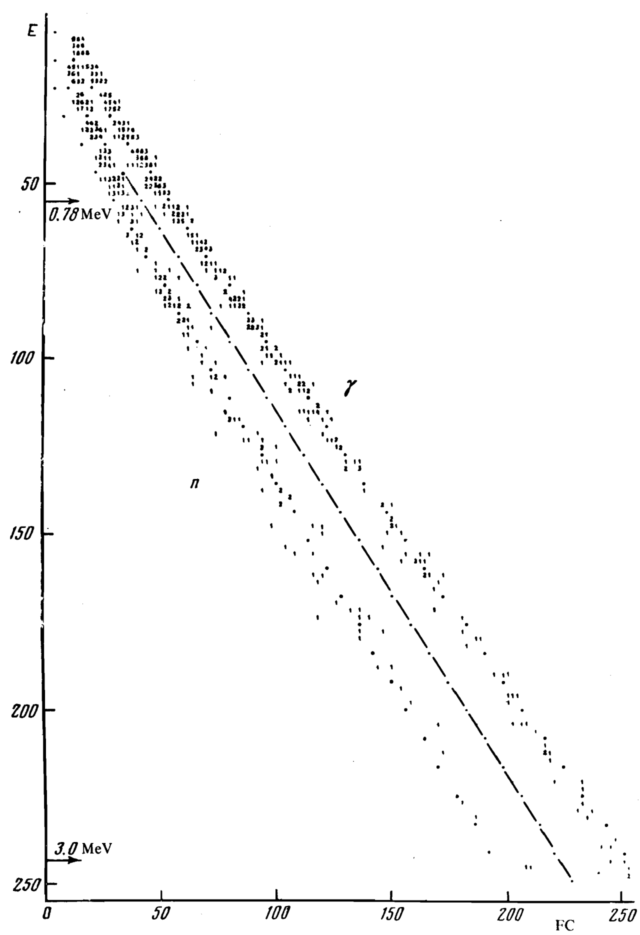

FIG. 3. Two-dimensional distribution (FC, E) obtained in calibration measurements with a Po-Be source for one of the neutron detectors. The abscissa is the channel number corresponding to the height of the FC pulse, and the ordinate is the channel number corresponding to the height of the signal E or equivalent electron energy. The points show the location found by computer for the lines of the centers of gravity of the nonrelativistic (n) and relativistic (γ) regions and also the location of their line of separation. The latter is shown in the figure by the dotdash line.

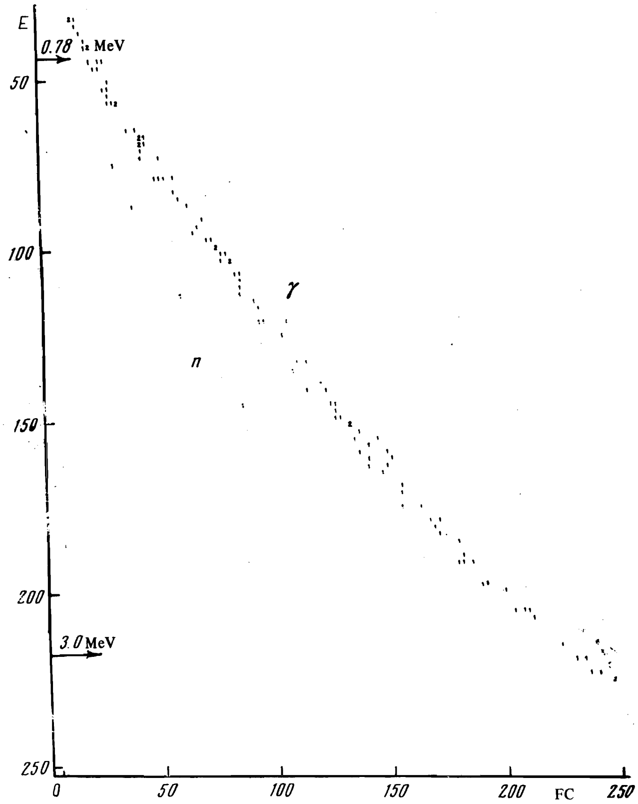

FIG. 4. The same as Fig. 3 but for the neutron portions of one of the series of measurements with hydrogen. The location of the lines of the centers of gravity of the regions and the line of their separation are not shown.

The ratio η_γ/η_n was determined in measurements with a mixture of hydrogen and xenon with a relative xenon concentration of 3×10^{-5}. Use of a mixture of these gases with this concentration is dictated by the following considerations. First, under these conditions intensive transfer of muons occurs from $p\mu$ atoms to xenon. The relative number of $Xe\mu$ atoms formed as the result of transfer is large (under our conditions 0.4) and therefore the yields of mesic x rays from $Xe\mu$ mesic atoms and of neutrons from muon capture in these mesic atoms can be measured with high accuracy. Second, xenon has an atomic number ($Z_{Xe} = 54$) lying between iodine ($Z_I = 53$) and cesium ($Z_{Cs} = 55$) and therefore the ratios of the γ-ray and neutron yields for these three elements should be about the same. (It is known that the energies of the K_α line of the mesic x rays for mesic atoms of these elements differ by no more than 3% (see, for example, ref. 26), and the yields and neutron spectra from μ capture in iodine, xenon, and cesium nuclei are practically identical.[24])

When these facts are taken into account,

$$(\eta_\gamma/\eta_n)_{CsI} \approx (\eta_\gamma/\eta_n)_{H+Xe} K_{geom} \quad (11)$$

where K_{geom} is a factor taking into account the difference in the ratios of the detection efficiencies for neutrons and γ rays under the conditions of "volume" (H + Xe) and "wall" (CsI) geometry. The value of K_{geom} calculated by computer is 0.93. Here the accuracy with which Eq. (11) is satisfied, according to our estimates, is 5% or better.

The results of the experiments to determine the background from diffusion of $p\mu$ atoms[3)] are given in Table IV. The number of muon stoppings N_μ was determined by measurement of the electron yield and by use of the detection efficiency ϵ_e given in Table II. The γ-ray yields are the experimental values after subtraction of the normalized background. This background (accidental coincidences and electron bremsstrahlung) was determined in special experiments with a target filled with pure helium.

TABLE IV. Data of experiments to determine background from diffusion

Quantity	Target filling	
	H	H + Xe
$N_\mu \cdot 10^{-6}$	5.07	1.60
$\eta_\gamma \cdot 10^6$	31±8	1020±34
η_γ/η_n	—	6.8±1.0

Using the data of Table IV for η_γ^H and η_γ/η_n together with Eqs. (10) and (11), we find the value of the background from diffusion, normalized to the number of muon stoppings. This value, multiplied by the total number of muon stoppings recorded in the neutron runs with hydrogen, is given in the third line of Table V.

7. ANALYSIS OF NEUTRON EVENTS

Data illustrating the analysis of the neutron events are given in Table V. For the purpose of separating the background (accidental coincidences and diffusion) the time distribution obtained for all 685 events was approximated by the following function:

$$dN_n/dt = Ae^{-\lambda_0 t} + B\varphi(t) + C, \quad (12)$$

where $\varphi(t)$ is the time dependence calculated by computer for neutrons arising from diffusion of $p\mu$ atoms to the walls, and C is the accidental coincidence level. In analysis of the time distribution we used the data which are given in the first three lines of Table V. The experimentally determined distribution is given in Fig. 5. In this figure the solid curve 1 corresponds to a function of the form of Eq. (12) with parameters determined by computer. The dashed lines 3 and 2 correspond to the accidental-coincidence level and an exponential with an argument $-\lambda_0 t$. It was found from a χ^2 analysis of the time distribution that the number of events belonging to the exponential with argument $-\lambda_0 t$ is 323 ± 32. This number includes both events from capture in hydrogen and background events arising as the result of photonuclear reactions in stilbene from bremsstrahlung photons.

To determine the background from photonuclear reactions we used the measured numbers of neutron events in the electron runs with hydrogen. From this number, on the basis of the data obtained in the neutron runs, we subtracted events due to muon capture in hydrogen, accidental coincidences, and diffusion of $p\mu$ atoms. The ratio of the difference obtained in this way to the number of muon stoppings recorded in the electron runs was interpreted as the yield of neutron events $\eta_n^e(\gamma, n)$ produced by (γ, n) and (γ, p) reactions in stilbene. For the neutron runs the yield found in this way was decreased by a number of times equal to the degree of discrimination against electrons[4)]:

$$\eta_n^{neutr}(\gamma, n) \approx \eta_H^e(\gamma, n)[1 - \varepsilon_e(5)]; \quad (13)$$

here $\epsilon_e(5)$ is the efficiency of detection by counter 5 of those electrons which fall in the solid angle of the neutron detectors. From the data given in Table III and Eq. (13) it was found that the contribution of neutron

TABLE V. Interpretation of neutron events

Parameter	Value
Total number of events	685±27
Accidental-coincidence level	66±4.3 μsec^{-1}
Neutrons from diffusion of $p\mu$ atoms	98±27
Neutron background from (γ, n) and (γ, p) reactions	45±6
Number of events from muon capture in hydrogen	278±33

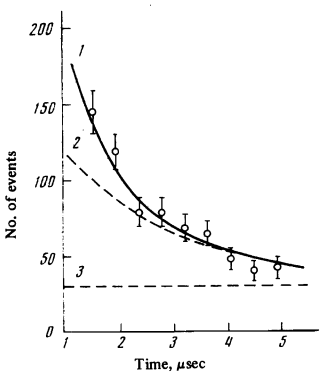

FIG. 5.

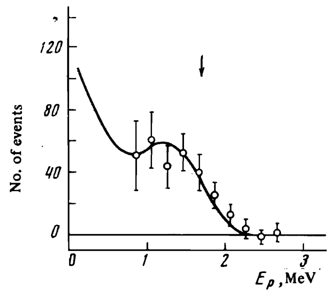

FIG. 6.

FIG. 5. Time distribution obtained for neutron events in runs with hydrogen. The abscissa is the time from the moment of stopping of the muon, and the ordinate is the number of events per interval of 0.433 μsec.

FIG. 6. Pulse-height spectrum of recoil protons, measured for events from capture of muons in hydrogen. The normalized background has been subtracted. The abscissa is the proton energy on the scale of the equivalent electron energy, and the ordinate is the number of events per interval of 0.2 MeV. The arrow indicates the expected location of the limiting energy in the proton spectrum for detection of neutrons from reaction (1).

events from photonuclear reactions in stilbene is 45 ± 6.

The final number of events due to capture of muons in hydrogen is given in the last line of Table V. The recoil-proton pulse-height spectrum obtained for events from capture in hydrogen is given in Fig. 6. The smooth curve in this figure corresponds to the computer-calculated normalized pulse-height distribution of neutrons from process (1).

8. DETERMINATION OF MUON CAPTURE RATE IN A pμ ATOM. DISCUSSION OF RESULTS

The muon capture rate in a pμ atom was determined by means of the expression

$$\lambda_{capt}^{p\mu}=\lambda_0\frac{N_n/\varepsilon_n}{N_e/\varepsilon_e}\frac{1}{\rho}. \quad (14)$$

Here $N_n = 278 \pm 33$ is the number of neutron events from μ capture in hydrogen. The quantity N_e was defined as

$$N_e=(N_e^e/M^e)M^{\text{neutr}}, \quad (15)$$

where N_e^e is the number of electron events, after subtraction of accidental coincidences, recorded in all electron runs and M^e and M^{neutr} are the total numbers of monitor pulses (23 coincidences) respectively in electron and neutron runs. The ratio N_e^e/M^e is the experimental electron yield measured in periodically repeated electron runs. These values are in good statistical agreement for all runs. The value obtained for N_e turned out to be $(1.863 \pm 0.008)\times 10^6$.

The detection efficiencies ϵ_n and ϵ_e are given in the last line of Table II. The uncertainties in these values include the statistical errors in the Monte Carlo calculations and the errors in the tabulated values of the cross sections for interaction of neutrons with matter, and also take into account the uncertainty in our knowledge of the thresholds in the pulse-height spectra of neutrons and electrons. The largest contribution (~3%) to the error ϵ_n is due to the uncertainties in the parameters of the expression for the equivalent energy of electrons in stilbene as a function of the proton energy.

The parameter ρ in Eq. (14) takes into account the fact that under our conditions μ capture occurs partly from the $(pp\mu)^+$ state of the mesic molecular ion. We used the averaged data of refs. 9–11 for the $(pp\mu)^+$ formation rate. The value of ρ was obtained by integration of the expression for the time resolution of neutrons from capture in $(pp\mu)^+$ with allowance for Eq. (6). It turned out to be $\rho = 0.943$.

The muon capture rate in a pμ atom found by us by means of Eq. (14) is

$$\lambda_{capt}^{p\mu}=686\pm88 \text{ sec}^{-1} \quad (16)$$

and is given in Table I. It can be seen that our data are in good agreement both with the results of ref. 7 and with the theoretical predictions. As is well known, calculations of λ_{capt} utilize the coupling constants g_V and g_A found in β decay. Therefore the agreement of the experimental data on μ capture in hydrogen with the theory confirms the hypothesis of a universal weak interaction.

From the theory it follows that for $g_V = 0$ the rate of occurrence of process (1) is ~400 sec^{-1}, and for $g_V = g_A$ it is about 200 sec^{-1}. Comparison of our experimental data with these calculations and also with the value (5) for $\lambda_{capt}^{p\mu}$ calculated for the V-A variant permits two additional important conclusions to be drawn: 1) that the vector (Fermi) interaction is present in μ capture and 2) that the V-A variant of the interaction is realized in this process.

We recall that the results on μ capture in complex nuclei are not very sensitive to the vector coupling constant.

The closeness of our data and the results of ref. 7 permits them to be combined, and this leads to the value

$$\lambda_{capt}^{p\mu}=661\pm48 \text{ sec}^{-1}. \quad (17)$$

Using the equation obtained by Frazier and Kim[3] for $\lambda_{capt}^{p\mu}$, we calculated this quantity for various values of the ratios g_A/g_V and g_P/g_A. The results of the calculations are shown in Fig. 7. The solid curve corresponds to the average value (17) and the dashed curves to the error corridor for this quantity. Figure 7 also shows the theoretical value $\lambda_{capt}^{p\mu}$ (the point) calculated by Frazier and Kim[3] for $g_A/g_V = -1.23$ and for the value $g_P/g_A = 7.3$ corresponding to the Gell-Mann and Levy version[27] of the theory in the so-called hypothesis of partially conserved axial current (PCAC).

If we set $g_A/g_V = -1.23$, then the range of allowed values for g_P/g_A follows from Eq. (17):

$$3.9\leqslant g_P/g_A\leqslant 9.0. \quad (18)$$

The theory gives $g_P/g_A \approx 7$, and the relative spread in the values of this quantity calculated in various versions[27,28] of the PCAC hypothesis or from the ordinary dispersion relations[29] is about 10%. As can be seen

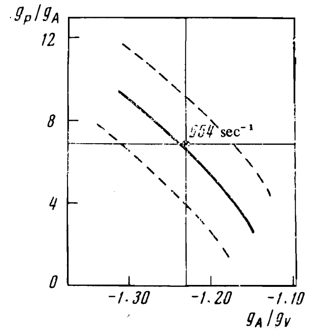

FIG. 7. Dependence of g_p/g_A on g_A/g_V corresponding to the experimental data (16), obtained by means of the expression for $\lambda^{p\mu}_{capt}$ given by Frazier and Kim[3] The point shows the theoretical value of $\lambda^{p\mu}_{capt}$ calculated by Frazier and Kim for $g_A/g_V = -1.23$ and for $g_p/g_A = 7.3$ obtained on the basis of ref. 27.

from Eq. (18), the experimental data at the present time do not permit an unambiguous choice to be made between the different theoretical models in which g_P is calculated.

Analysis of the experimental data for Eq. (17) permits us to conclude that they agree with the theoretically predicted renormalizability of the weak interaction constants for process (1), although the data do not yet permit a detailed verification to be made of the nature of the dependence of these constants on the momentum transfer.

The authors express their sincere appreciation to V. I. Salatskiĭ, I. V. Sizov, and I. A. Chepurchenko for assistance in making the calibration measurements in the 5-MeV electrostatic generator, to V. G. Zinov and A. D. Konin for providing the γ spectrometer and for numerous discussions, to V. S. Evseev and T. N. Mamedov for discussion of the data on the yield and spectra of neutrons in μ capture in nuclei, to S. S. Gershteĭn, Yu. M. Kazarinov, and R. A. Eramzhyan for frequent discussions of the results of this work, to S. V. Medved' and E. B. Ozerov for providing trouble-free operation of the measurement center and computer, to E. I. Rozanov for highly efficient operation of the synchrocyclotron, and also to M. M. Kuznetsov and Sh. G. Shamsutdinov for assistance in building the experimental equipment and making the measurements.

1)Institute of High Energy Physics, Serpukhov.

2)In the two-dimensional (FC, E) distributions, events corresponding to detection of relativistic particles (γ rays and electrons) and nonrelativistic particles (neutrons and protons) were placed in two different regions.[19]

3)On the basis of these data we also determined the cross section for elastic scattering of $p\mu$ atoms by protons, which turned out to agree with our earlier measurements of this quantity[15] and to exceed by more than an order of magnitude the theoretical values.[14]

4)It can be shown that Eq. (13) is valid at least whithin 15%.

[1] H. Primakoff, Rev. Mod. Phys. 31, 802 (1959).

[2] P. K. Kabir, Z. Phys. 191, 447 (1966).

[3] J. Frazier and C. W. Kim, Phys. Rev. 177, 2568 (1969).

[4] R. H. Hildebrand, Phys. Rev. Lett. 8, 34 (1962).

[5] E. Bertolini, A. Citron, G. Gianella, S. Focardi, A. Mukhin, C. Rubbia, and F. Saporetti, Proc. Int. Conf. on High Energy Physics, Geneva, 1962.

[6] J. E. Rothberg, E. W. Anderson, E. J. Bleser, L. M. Lederman, S. L. Meyer, J. L. Rosen, and I-T. Wang, Phys. Rev. 132, 2664 (1963).

[7] A. Alberigi Quaranta, A. Bertin, G. Matone, F. Palmonari, G. Torelli, P. Dalpiaz, A. Placci, and F. Zavattini, Phys. Rev. 177, 2118 (1969).

[8] C. J. Christensen, A. Nielsen, A. Bahnsen, W. K. Brown, and B. M. Rustad, Phys. Rev. 5D, 1628 (1972).

[9] G. Conforto, C. Rubbia, E. Zavattini, and S. Focardi, Nuovo Cimento 33, 1001 (1964).

[10] E. J. Bleser, E. W. Anderson, L. M. Lederman, S. L. Meyer, J. L. Rosen, J. E. Rothberg, and I-T. Wang, Phys. Rev. 132, 2679 (1963).

[11] Yu. G. Budyashov, P. F. Ermolov, V. G. Zinov, A. D. Konin, A. I. Mukhin, and K. O. Oganesyan, JINR Preprint R15-3964, Dubna, 1968.

[12] Ya. B. Zel'dovich and S. S. Gershteĭn, Zh. Eksp. Teor. Fiz. 35, 649 (1958) [Sov. Phys. 8, 451 (1959)]. S. Weinberg, Phys. Rev. Lett. 4, 575 (1960).

[13] W. R. Wessel and P. Phillipson, Phys. Rev. Lett. 13, 23 (1964). A. Halpern, Phys. Rev. 135, A34 (1964).

[14] S. S. Gershteĭn, Zh. Eksp. Teor. Fiz. 34, 463 (1958) [Sov. Phys.-JETP 7, 318 (1958)]. Ya. B. Zel'dovich and S. S. Gershteĭn, Usp. Fiz. Nauk 71, 581 (1960) [Sov. Phys.-Uspekhi 3, 593 (1961)]. A. E. Ignatenko, L. B. Egorov, B. Khalupa, and D. Chultem, Zh. Eksp. Teor. Fiz. 35, 894 (1958) [Sov. Phys.-JETP 8, 621 (1959)].

[15] V. P. Dzhelepov, P. F. Ermolov, and V. V. Fil'chenkov, Zh. Eksp. Teor. Fiz. 49, 393 (1965) [Sov. Phys.-JETP 22, 275 (1966)].

[16] V. M. Bystritskiĭ, V. P. Dzhelepov, N. I. Doronicheva, P. F. Ermolov, K. O. Oganesyan, M. N. Omel'yanenko, S. Yu. Porokhovoĭ, A. A. Rodina, V. E. Teplov, and V. V. Fil'chenkov, Prob. Tekh. Eksp. 2, 226 (1972) [Instrum, Exp. Tech. 15, 576 (1972)].

[17] V. M. Bystritskiĭ, V. P. Dzhelepov, P. F. Ermolov, L. S. Kotova, V. I. Lepilov, K. O. Oganesyan, M. N. Omel'yanenko, S. Yu. Porokhovoĭ, A. I. Rudenko, and V. V. Fil'chenkov, Report JINR, 13-7246, Dubna, 1973.

[18] V. M. Bystritskiĭ, V. P. Dzhelepov, P. F. Ermolov, K. O. Oganesyan, M. N. Omel'yanenko, S. Yu. Porokhovoĭ, and V. V. Fil'chenkov, Prib. Tekh. Eksp., 4, 86 (1971) [Instrum. Exp. Tech. 14, 1047 (1972)].

[19] V. M. Bystritskiĭ, V. P. Dzhelepov, P. F. Ermolov, K. O. Oganesyan, M. N. Omel'yanenko, S. Yu. Porokhovoĭ, and V. V. Fil'chenkov, Prib. Tekh. Eksp., 1, 65 (1972) [Instrum. Exp. Tech. 15, 67 (1972)].

[20] A. N. Sinaev, A. A. Stakhin, and N. A. Chistov, Report, JINR, 13-4835, Dubna, 1969.

[21] S. G. Basiladze, P. F. Ermolov, and K. O. Oganesyan, Zh. Eksp. Teor. Fiz. 49, 1042 (1965) [Sov. Phys. JETP 22, 725 (1966)]. A. Placci, E. Zavattini, A. Bertin, and A. Vitale, Nuovo Cimento 64A, 1053 (1969).

[22] V. P. Dzhelepov, P. F. Ermolov, E. A. Kushnirenko, V. I. Moskalev, and S. S. Gershteĭn, Zh. Eksp. Teor. Fiz. 42, 439 (1962) [Sov. Phys.-JETP 15, 306 (1962)].

[23] A. Bertin, M. Bruno, A. Vitale, A. Placci, and E. Zavattini, Lett. Nuovo Cim. 4, 449 (1971).

[24] B. Macdonald, J. Diaz, S. Kaplan, and R. V. Pyle, Phys. Rev. 139B, 1523 (1965). V. S. Evseev and T. N. Mamedov, JINR Preprint R15-7115, Dubna, 1973.

[25] W. C. Barber, W. D. George, and D. D. Reagan, Phys. Rev. 98, 73 (1955). V. J. Vanhuyse and W. C. Barber, Nucl. Phys. 26, 233 (1961). V. Emma, C. Milone, and A. Rubbino, Phys. Rev. 118, 1297 (1960).

[26] G. Backenstoss, K. Goebel, B. Stadler, U. Hegel, and D. Quitmann, Nucl. Phys. 62, 449 (1965).

[27] M. Gell-Mann and M. Levy, Nuovo Cimento 16, 705 (1960). Chou Kuang-choo, Zh. Eksp. Teor. Fiz. 39, 703 (1960) [Sov. Phys.-JETP 12, 492 (1961)].

[28] Y. Nambu, Phys. Rev. Lett. 4, 380 (1960).

[29] L. Wolfenstein, Nuovo Cimento 8, 882 (1958). M. L. Goldberger and S. B. Treiman, Phys. Rev. 110, 1178 (1958).

Translated by C. S. Robinson
5